A two-layer predictive control for hybrid electric vehicles energy management

Nicoleta Stroe, Sorin Olaru, Guillaume Colin, Karim Ben-Cherif, Yann Chamaillard

A two-layer predictive control for hybrid electric vehicles energy management

Nicoleta Stroe [*] **Sorin Olaru** [**] **Guilaume Colin** [***]
Karim Ben-Cherif [*] **Yann Chamaillard** [***]

[*] *Renault SAS, Lardy, France, (e-mail:* $\{nicoleta - alexandra.stroe, karim.ben - cherif\}$*@renault.com)*
[**] *Laboratory of Signals and Systems, CentraleSupélec-CNRS-Univ. Paris-Sud, Univ. Paris-Saclay, Gif-sur-Yvette, (e-mail:sorin.olaru@centralesupelec.fr)*
[***] *Univ. Orléans, PRISME, France, (e-mail:*$\{guillaume.colin, yann.chamaillard\}$*@univ-orleans.fr)*

Abstract: In this paper, a two-layer predictive energy management strategy for hybrid electric vehicles without an external recharge is introduced. The low-level layer exploits telemetry data over a short-term horizon in a model predictive control structure that provides the engine torque, but also the stop-start decision. The upper layer uses a tuning mechanism with a longer horizon to calculate the MPC weighting factor that ensures a balance between the fuel and battery consumption. An analysis of this upper-level tuning prediction horizon dependence on the drive cycle characteristics is performed. The robustness with respect to state-of-charge and engine torque estimation is also proven by a sensitivity analysis.

Keywords: hybrid electric vehicle, energy management, predictive control

1. INTRODUCTION

Fuel consumption optimization is a priority objective in the automotive research, whose development during the last years has witnessed an increased interest in hybrid vehicles. The research work spans several fields related to this topic: topology, dimensioning, modeling and control. The latter tackles especially the energy management problem, which refers to the power distribution between the engine and the additional power source.

There are currently numerous techniques in the literature for the power distribution problem: dynamic programming (off-line solution, it needs the entire drive cycle), rule-based (Goerke et al., 2015), *Equivalent Consumption Minimization Strategy* (ECMS), with its different approaches, such as Adaptive-ECMS (Musardo et al., 2005) and Telemetric-ECMS (Sciarretta et al., 2004). Model predictive control (MPC) has gained in popularity during the last years, it its deterministic form (Cairano et al., 2011), (Lu et al., 2013) or stochastic (Ripaccioli et al., 2010), (Josevski and Abel, 2014).

Current technologies allow the acquisition of future traffic data and consequently, their exploitation within predictive control strategies, with explicit reconstruction of the speed profile or by the use of pattern recognition (drive cycle profile, driving style). In (Bender et al., 2014) the future target speed is reconstructed from the vehicle current position and a database, whereas in (Mayr et al., 2011) a cycle detection based on correlation analysis is performed. The ability to capture transient characteristics, such as abrupt changes, makes the frequency analysis a suitable approach: in (Wang et al., 2012) a wavelet-based analysis is used for feature extraction from accelerometer data, whereas in (Liu et al., 2015) a metric that characterizes speed fluctuations is defined using Fourier analysis.

This paper continues the previous work (Stroe et al., 2016b), where an MPC - based torque split optimization including stop-start mechanism has been introduced. It is assumed that the vehicle speed can be foreseen up to several kilometers and this prediction will be incorporated into a two-layer control structure, that work with longer horizons for the higher decision layers. The low-level controller handles the power distribution, which is reduced to torque calculation in the absence of gearshift optimization, and also the stop-start command. This problem is formulated as an MPC optimization, whose tuning parameter is calculated at the upper level, that uses a long-term prediction. The main contribution of this paper is to present a method to calculate the penalty factor in the MPC design as a sum of an average-based feedforward component, calculated over a prediction horizon, and a SOC feedback corrective term. The influence of the prediction horizon on fuel gain is analysed for different drive cycles. The robustness with respect to torque and SOC estimation is equally performed in order to complete the sensitivity analysis of the proposed structure.

The paper is organized as follows: first, a powertrain control-oriented model is introduced and next, an MPC formulation is presented, for the torque distribution and ICE stop-start, with a focus on the MPC tuning method. The performance and robustness of the proposed strategy are evaluated into a model-in-the-loop validation.

NOTATIONS

- ICE - Internal Combustion Engine
- EM - Electric Machine
- DCT - Dual-Clutch Transmission
- R_i - gear ratio engaged on i^{th} shaft (includes neutral definition), $i \in \{1 : odd, 2 : even\}$
- C_i - clutch status (0 - open, 1 - closed)
- $N_i = \min(R_i, 1)$ - used to define the case where one of the shafts is decoupled
- $R_{f(R_i)}$ - axle ratio corresponding to ith shaft
- $r^w_{ice/em}$ - ratio between the ICE/EM torque at wheel level and the component (ICE/ EM) torque
- rat_{em} - ratio between the EM and the corresponding shaft where it is connected
- ω^{ctrl}_{ice} - idle speed or 0 rpm, in case of engine stop
- R_w - wheel radius

2. POWERTRAIN CONTROL-ORIENTED MODEL

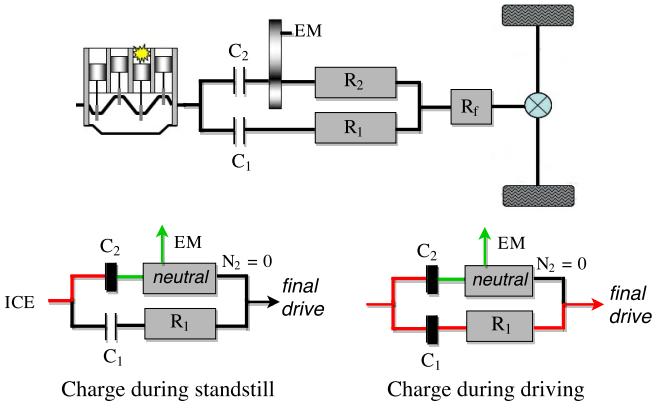

Fig. 1. DCT hybrid configuration

Vehicle dynamics is expressed using a backward approach, where the reference speed and acceleration are known and from which the required torque can be determined. Hence, the wheel torque demand can be calculated from the velocity (v), environment data, such as slope (α), air density (ρ_{air}) and vehicle parameters, such as the mass (m), frontal area (A_f), aerodynamic drag coefficient (c_d), rolling friction coefficients (c_{r0}, c_{r1}):

$$T_w = \Big(\frac{1}{2}\rho_{air}A_f c_d v^2 + (c_{r1}v + c_{r0})mgcos(\alpha) + mgsin(\alpha) + m\dot{v}\Big)R_w \quad (1)$$

A wheel level supervisory control is the most appropriate for an HEV, where the EM can be connected to different driveline positions. Shafts inertias and clutch dynamics are neglected and, therefore, a static model for torque and rotational speeds of the components is introduced, as in (2)-(6). The purpose of the model is to define a relation between the components torques and the total torque demand and for the rotational speeds, a dependence of velocity and driveline states (clutches states and gear engaged).

The architecture considered here is a dual-clutch transmission hybrid with the EM connected to the even primary shaft, as in Fig. 1. In (Stroe et al., 2016a) it was shown

Table 1. Hybrid DCT modes as functions of clutches states and N_2

C_1	C_2	N_2	*Case*
0	0	0	standstill, sailing
0	0	1	electric driving, regenerative braking
0	1	1	hybrid or conventional, even gear engaged
0	1	0	charge during standstill
1	0	0	conventional driving, odd gear engaged
1	0	1	hybrid driving
1	1	0	take-off, charge during driving

that with a proper parametrization, this configuration can represent all types of hybrid parallel architectures. For a better understanding of the system and of the proposed model, Table 1 summarizes the clutches states with respect to functional modes. The variable N_2 is introduced in order to correctly define special cases when one of the shafts is decoupled from the wheel (to charge the battery via the ICE at standstill or during driving, with odd gear engaged). For the present configuration, only the even shaft is concerned, due to EM position. The engine is disconnected from the drive not only for the case when $C_1 = C_2 = 0$, but also for the charge at standstill, where $C_2 = 1$, but $N_2 = 0$. Therefore, the ICE speed will be defined by ω^{ctrl}_{ice} when $C_1 + N_2C_2 = 0$, as expressed in (5).

$$T_w = r^w_{ice}T_{ice} + r^w_{em}T_{em} \quad (2)$$

$$r^w_{ice} = R_{f_{(R_1)}}R_1C_1 + R_{f_{(R_2)}}R_2C_2 \quad (3)$$

$$r^w_{em} = R_{f_{(R_1C_1C_2+R_2)}}(R_1C_1C_2 + R_2)\,rat_{em} \quad (4)$$

$$\omega_{ice} = r^w_{ice}\frac{v}{R_w} + (1 - C_1 - N_2C_2)\,\omega^{ctrl}_{ice} \quad (5)$$

$$\omega_{em} = r^w_{em}\frac{v}{R_w} + rat_{em}C_2\,(1 - C_1)\,(1 - N_2)\,\omega^{ctrl}_{ice} \quad (6)$$

The battery SOC is the only considered state of the system, for which an internal resistance model has been retained in this paper. Its dynamics is described by the integrator-like relation below, involving its open circuit voltage (OCV), internal resistance (R), battery capacity (Q_{max}).

$$\dot{SOC} = -\frac{OCV_{(SOC)} - \sqrt{OCV^2_{(SOC)} - 4R_{(SOC)}P_b}}{2R_{(SOC)}Q_{max}} \quad (7)$$

where $P_b = \frac{\pi}{30}\omega_{em}T_{em} + loss\,(\omega_{em}, T_{em})$ is the battery power.

The engine fuel rate is given as a non linear map with respect to torque and rotational speed, but in view of control design, an analytical expression with an explicit appearance of the control variable, is needed. The vehicle considered for this case-study is equipped with a turbo-charged 1.2 L SI engine, whose fuel rate dependence on torque is illustrated in Fig. 2, via a parametrization of curves with respect to ω_{ice}. In this paper, a piecewise linear approximation with respect to torque is introduced, as expressed below:

$$\dot{m}_f = \alpha_j(\omega_{ice})T_{ice} + \beta_j(\omega_{ice}), \quad \text{for } j = 1 \dots N_{part} \quad (8)$$

where N_{part} is the number of torque partitions.

3. MPC- BASED ENERGY MANAGEMENT

The focus of this work is the optimization-based decision making for torque distribution between the engine and the electric machine with respect to fuel consumption, for a

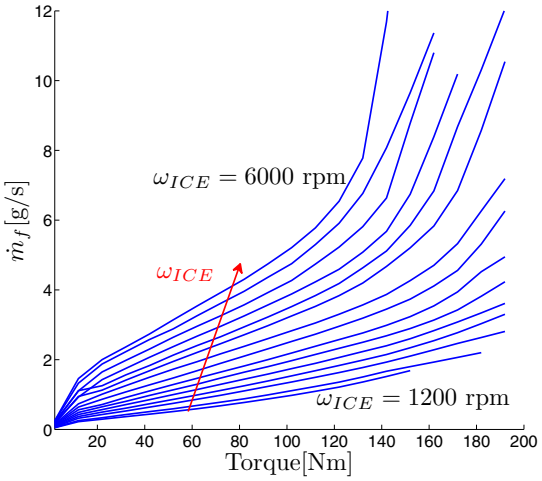

Fig. 2. Fuel consumption [g/s] with respect to torque; curves for different engine speeds

hybrid vehicle without an external recharge. It is assumed that the future vehicle speed profile can be extracted from the navigation data system for a preview distance of several kilometers.

3.1 Optimization criterion

The choice of the cost function should reflect the trade-off between fuel and battery consumption. A local fuel-friendly strategy would be to use the battery as much as possible, but the absence of an external recharge would imply to charge the battery later, via the engine, if the regenerative braking phases are not enough. A cost function defined as a weighted sum of the two power sources is given by PMP (Pontryagin's Minimum Principle):

$$\begin{aligned} &\min_{u_k} P_{f_k} + \lambda_k P_{e_k} \\ &P_{f_k} = H_{LV}\dot{m}_{f_k}, \quad P_{e_k} = OCV_k S\dot{O}C \end{aligned} \tag{9}$$

where k is the current step, H_{LV} is the lower heating value of the fuel, u_k is the engine torque and λ_k is a penalty, usually called equivalence factor. The choice of the optimization criterion in the present developments is inspired from the above design, but with the squared values of the powers:

$$\min_{u} \sum_{i=k}^{k+N_{MPC}-1} P_f^2(i) + \lambda_k^2 \left(P_{e_k}(i) - P_{emin_k}(i)\right)^2 \tag{10}$$

where N_{MPC} is the prediction horizon, u is a vector with ICE torques of length N_{MPC} and P_{emin_k} is the electrochemical power minimal value. This latter element is used as a displacement term, in order to properly include the sign information of the electrochemical power, that would otherwise be lost if only the squared value were used.

3.2 Problem formulation

As mentioned in the first section, the only system dynamics is the battery SOC, whose nonlinear model is defined by (7). In this work, a linearisation at the operating point is introduced, resulting into a Linear Time-Varying (LTV) prediction model:

$$x_{k+1} = x_k + B_k u_k + D_k \tag{11}$$

where $x = SOC, u_k = T_{ICE}(k)$, D_k is a residual term due to linearisation. It can be noticed that the model is representing practically an integrator-like dynamics, with B_k and D_k time-varying, dependent on wheel torque demand $T_w(k)$ and EM rotational speed $\omega_{EM}(k)$. The variations of open circuit voltage and internal resistance with respect to SOC are neglected during the prediction. With this simplification, the optimization problem introduced before can be formulated as a quadratic programming:

$$\min_{U} \quad \frac{1}{2}U^T H U + F^T U \tag{12a}$$

$$\text{s.t.} \begin{cases} A_{ineq} U \leq b_{ineq} \\ A_{eq} U = b_{eq} \end{cases} \tag{12b}$$

With the definitions from (9) and (8), the expressions of the matrices involved in the QP formulation are given below:

$$H_k = \bar{\alpha}_k^2 + q_k^2 \bar{B}_k^2 \tag{13a}$$

$$F_k = \bar{\alpha}_k \bar{\beta}_k - q_k^2 \bar{B}_k U_k^{max} \tag{13b}$$

where $q_k = \lambda_k \frac{1}{H_{LV}} Q_{max} OCV_k, \quad \bar{B}_k = diag\left(B_{k+i-1}\right),$

$$\bar{\alpha_k} = \begin{bmatrix} \alpha_{j_1}\left(\omega_{ice_k}\right) & \cdots & 0 \\ \vdots & \ddots & \vdots \\ 0 & \cdots & \alpha_{j_{N_{mpc}-1}}\left(\omega_{ice_{k+N_{mpc}-1}}\right) \end{bmatrix},$$

$$\bar{\beta_k} = \begin{bmatrix} \beta_{j_1}\left(\omega_{ice_k}\right) & \cdots & \beta_{j_{N_{mpc}-1}}\left(\omega_{ice_{k+N_{mpc}-1}}\right) \end{bmatrix},$$

where the index j_i denotes the fuel consumption region j (8) for the ith element in the array U_k and U_k^{max} is an array with the control upper bounds.

The constraints are defined with respect to physical limitations of torque and power, but the SOC balance problem needs to be handled separately. For a hybrid without an external recharge, it is usually imposed to have at the end at the drive cycle the same SOC value as in the beginning. In this way, a fair comparison with a conventional vehicle or between different strategies can be done. The solution proposed here is the use of distance-varying limits:

$$\begin{aligned} SOC_k^{min} &= SOC_0 - (SOC_0 - SOC_{min})\, e^{1-\frac{1}{1-\frac{d_k}{d_{Tot}}}} \\ SOC_k^{max} &= SOC_0 + (SOC_{max} - SOC_0)\, e^{1-\frac{1}{1-\frac{d_k}{d_{Tot}}}} \end{aligned} \tag{14}$$

where SOC_{min}, SOC_{max} are the physical lower and upper bound (usually take values of 20% and 90%, respectively), d_k is the current distance and d_{Tot} is the drive cycle total distance. The purpose is to force the SOC trajectory to approach the initial value, as the vehicle reaches its destination. This condition implies the knowledge of the total distance, which is not always realistic. An alternative is the use of a reset distance, as depicted in Fig. 3. In simulation, this can be set to standard drive cycles distance, but in practice it can be extracted from the driver's history data. The constraints are hence expressed as below:

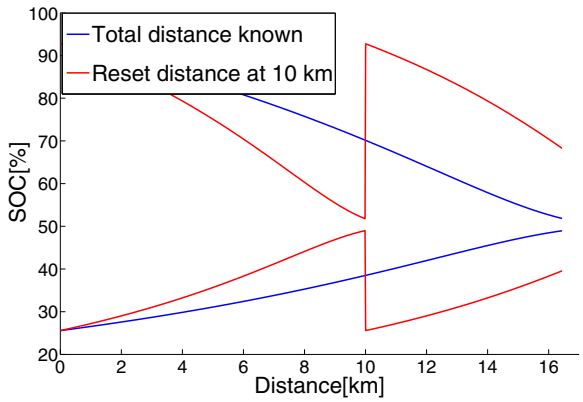

Fig. 3. SOC limits for 2 cases: total distance known and reset distance fixed at 10 km, respectively

$$T_{ice}^{min}(\omega_{ice}) \leq T_{ice} \leq T_{ice}^{max}(\omega_{ice}) \quad (15a)$$
$$T_{em}^{min}(\omega_{em}) \leq T_{em} \leq T_{em}^{max}(\omega_{em}) \quad (15b)$$
$$P_{em}^{min}(\omega_{em}) \leq \frac{\pi}{30}\omega_{em}T_{em} \leq P_{em}^{max}(\omega_{em}) \quad (15c)$$
$$SOC_k^{min} - \epsilon_k \leq X_k \leq SOC_k^{max} + \epsilon_k \quad (15d)$$

where ϵ_k is a slack variable used to soften the constraints, in order to avoid infeasibility problems that may occur when SOC variation range is too narrow.

3.3 ICE stop-start strategy

It is assumed that the drivelines states (gears and clutches) are calculated at the supervisory level and used as inputs by the MPC controller. The ICE can be stopped during standstill and regenerative braking, but also during pure electric traction. The inclusion of stop-start functionality makes the optimization more complex due to the discrete nature of the problem. In order to avoid the introduction of an additional optimization variable, an *a-posteriori* stop decision based on the sequence of calculated future commands is introduced here.

Let t_{idle} be the number of seconds of idling that translate the cost of a restart, Δt_{opt} the MPC sampling time and ct_{on} the number of steps after an ICE restart. Then, the condition to stop the engine is given by:

$$U_k\,(1 : N_{stop}) \leq T_{ice}^{thr} \quad (16a)$$
$$ct_{on} > N_{start} \quad (16b)$$

where $N_{stop} = \frac{t_{idle}}{\Delta t_{opt}}$ and T_{ice}^{thr} is an ICE torque threshold below which is preferable to stop the engine. The condition (16b) is introduced in order to avoid frequent stops. With this approach, the cost of a restart is implicitly included by the length of the considered subsequence of commands.

The access to a sequence of future commands allows the N_{on} - step restart anticipation, in order to improve speed tracking. If the value of the command on the position $1 + N_{on}$ exceeds the ICE torque threshold, then a restart command is activated. For the current study, a sampling time of 0.5 s is used and thus, N_{on} is set to 1.

4. TUNING METHOD

The penalty factor λ has a tremendous impact on the performance and the main difficulty of tuning arises from its dependence on the drive cycle. Given the lower and upper bound of the command at each predicted step i, the solution explored in the present study is to express λ as a ratio of the 2 powers variations between these bounds, as expressed below, where k is the optimization step:

$$\lambda_{k,i} = -\frac{P_f(\overline{u}_{k,i}) - P_f(\underline{u}_{k,i})}{P_e(\overline{u}_{k,i}) - P_e(\underline{u}_{k,i})} \quad (17)$$

Moreover, the navigation data system can provide information about future traffic conditions over a longer horizon than the one used for MPC. Thus, the proposed solution can use an average-based calculation over this penalty-adaption horizon, in combination with a proportional feedback SOC control:

$$\lambda_k = \frac{1}{N_\lambda - N_\lambda^{stop}} \sum_{i=k}^{k+N_\lambda-1} \lambda_{k,i} + k_r\,(SOC_{sp} - SOC_k)$$
$$N_\lambda^{stop} \text{ - number of predicted steps of vehicle standstill}$$
$$SOC_{sp} \text{ - SOC setpoint} \quad (18)$$

where $\lambda_{k,i}$ is given by (17). The expression contains therefore, 2 terms: a feed-forward component (the average in $\lambda_{k,i}$) and a feedback part (the proportional SOC control). The purpose of the latter is to adjust the penalty factor with respect to an SOC setpoint:

- if the trajectory is below the setpoint, λ increases, thus penalizing more the use of the battery
- if the trajectory is greater than the reference, λ will diminish and this will be translated into a greater use of the battery.

In this case, the setpoint was chosen constant and equal to the initial value. The goal is not to track a certain SOC reference, but to allow the trajectory to freely vary and to avoid overcharge or discharge.

The braking phases need to be included in the average calculation, but in this case $\lambda_{k,i}$ can no longer be expressed as a ratio of differences, because these modes are pre-imposed: the maximum possible energy is recovered and the rest is dissipated in the friction brakes. Therefore, a particular relationship is adopted in the present study:

$$\lambda_{k,i} = \frac{P_f^{idle}}{P_e^{regen}(k|k+i)}, \quad \text{for } T_w(k+i) < 0 \quad (19)$$

where $P_f^{idle} = H_{LV}\dot{m}_f^{idle}$ and $P_e^{regen}(k|k+i)$ is the predicted electrochemical power obtained by regenerative braking.

With this formulation λ will decrease if braking phases are anticipated. Thus, the use of the electric motor is encouraged if is possible to compensate the electric consumption by regenerative braking.

4.1 Choice of the horizon in the tuning procedure

The feed-forward component should encapsulate the trade-off between general tendency and aggressiveness of the drive cycle along a receding window. The longer the horizon N_λ, the smoother the feed-forward component becomes. MPC performs a local optimization and therefore, λ should be able to adapt fast enough with respect to

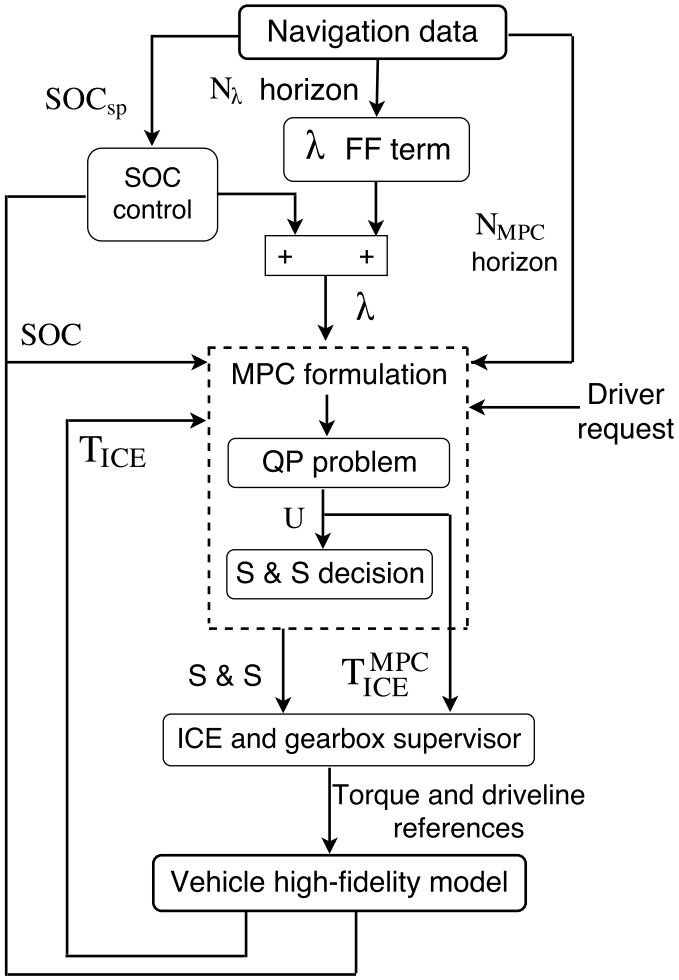

Fig. 4. Generic representation of the control structure; in present study, SOC_{sp} was set constant. $S\&S$ stands for stop & start

drive cycle aggressiveness. In (Liu et al., 2015), a measurement of traffic and driver aggressiveness based on jerk periodograms has been introduced. The periodogram is an estimate of the spectral density and it is given by the squared modulus of the Discrete Fourrier Transform.

In this paper, the periodogram of the wheel power will be used to analyse the aggressiveness information incorporated into λ, by using the frequency cumulative content for different prediction horizon values as in the expression below, where p stands for periodogram.

$$r = \frac{\int_{f=0}^{\frac{1}{2}f_{N_\lambda}} p(f)df}{\int_{f=0}^{\frac{f_s}{2}} p(f)df} \tag{20}$$

where f_s is the sampling frequency (here: $f_s = 1$Hz), $f_{N_\lambda} = \frac{1}{N_\lambda}$. This definition implies that for $N_\lambda = 1$s, the ratio is 1, that is, all drive cycle variations are included because no averaging is performed. If N_λ increases, the ratio diminishes due to smoothing. This can be observed in Fig. 5, where the evolution of the aggressiveness indicator with respect to the prediction horizon is depicted for several drive cycles. For values superior to 60s, the smoothing is significant for all the scenarios considered. In certain cases, such as ARTEMIS urban and traffic jam, the loss of aggressiveness information occurs at even lower horizons

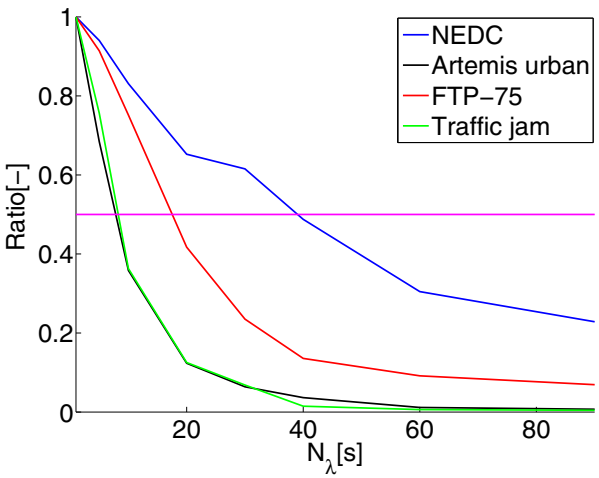

Fig. 5. Ratio of the frequency content for different prediction horizon values and drive cycles

and therefore, the prediction horizon choice is drive - cycle dependent.

5. SIMULATION AND RESULTS

The strategy was validated in Matlab/Simulink, in co-simulation with a high-fidelity model for the vehicle, designed in AMEsim. The cost of a restart was set to $t_{idle} = 2$s, MPC sampling time $\Delta t_{opt} = 0.5$s and thus, $N_{stop} = 4$. Several drive cycles were considered, whose speed profiles are depicted in Fig. 6.

The influence of the upper layer horizon was analyzed for a MPC control horizon of 5s which is long enough to include the stop-start decision (Stroe et al., 2016b). The consumption sensitivity with respect to N_λ is illustrated in Fig. 7. NEDC shows a decrease in consumption until $N_\lambda = 40$s and then, an increase (final SOC is the same for all the cases). For Artemis urban, $N_\lambda = 5$s gives the lowest normalized consumption, for a final SOC slightly greater than the one for the other horizons ($SOC_f = 52.58\%$ for $N_\lambda = 5$s vs $SOC_f = 51.15\%$ for the other values). FTP-75 shows an improvement up to 20s, and then a constant degradation, with a final SOC that slightly decreases starting with N_λ. For the traffic jam, an horizon of 10s provides the lowest consumption value, with a non-monotonic behavior for the higher horizons.

These results can be interpreted through the aggressiveness analysis introduced in the previous section. From Fig. 5 it is possible to extract a limit for the upper layer horizon and its optimal value can be determined by empirically choosing the value of 0.5 for the ratio defined by (20), which would translate the trade-off between average and transient behavior. This gives $N_\lambda = 40$s for NEDC, 5s for Artemis urban, 20s for FTP-75 and 10s for traffic jam. The values are therefore around 30s, which is coherent with the current availability of accurate preview data.

A comparison with a PMP - based method, as defined in (9), is summarized in Table 2, where for the MPC strategy the N_λ with the best consumption was retained. In PMP case, a constant equivalence factor was determined offline

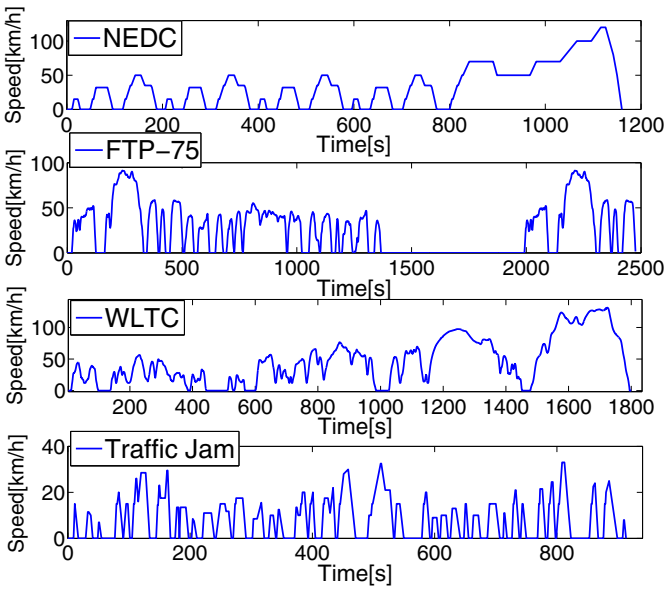

Fig. 6. Speed profile for different drive cycles

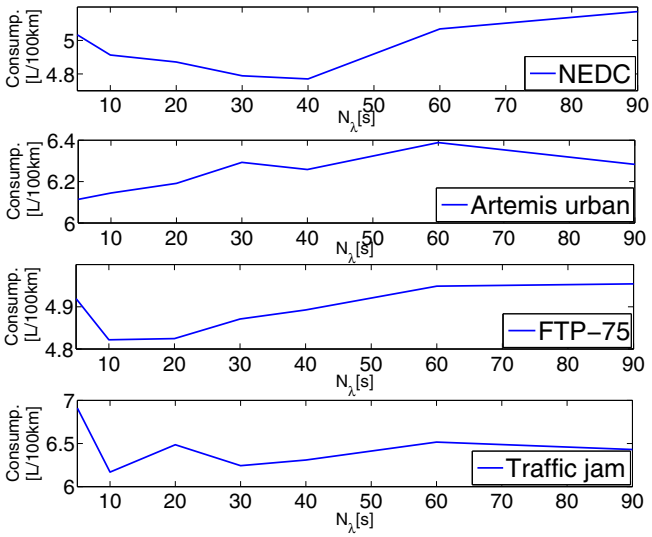

Fig. 7. Evolution of the normalized consumption w.r.t. N_λ for different drive - cycles

Table 2. Fuel consumption [L/100km] and final SOC[%], PMP and MPC

Strategy / Cycle	PMP	MPC	Relative difference
NEDC	4.5 (70.26%)	4.76 (70.57%)	5.77%
Artemis urban	5.61 (52.76%)	6.11 (52.58%)	8.9%
FTP-75	4.5 (55.74%)	4.82 (55.16%)	7.11%
Traffic jam	5.55 (50.12%)	6.16 (50.32%)	11%

for each drive cycle while the engine stop was performed for the electric traction phases.

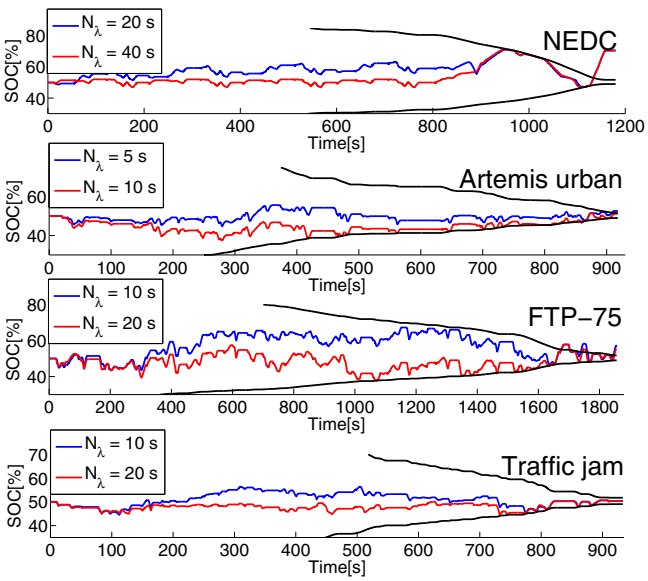

Fig. 8. SOC trajectories for 2 different N_λ; black curves represent SOC limits

5.1 Robustness analysis

The MPC controller, as shown in Fig. 4, receives at each optimization step the estimated engine torque and the battery SOC from the vehicle high-fidelity model. The former is used in the model linearization at the operating point and the latter represent the current state which interferes in the calculation of the model parameters (OCV and R in (7)) and also in the feedback correction term of the penalty factor. The technical specifications state that the SOC can be estimated with a precision of $\pm 1\%$ of its value, whereas for the torque, the estimation accuracy is of $\pm 5\%$. For each drive cycle, the 5 scenarios listed below have been considered and the results summarized in Tables 3 and 4 for two different N_λ values.

(1) positive offset for T_{ice}, accurate SOC
(2) negative offset for T_{ice}, accurate SOC
(3) signed offset for T_{ice}, but with a random distribution, accurate SOC
(4) random offset of $\pm 1\%$ of its current value for SOC, accurate T_{ice}
(5) random offsets on both inputs

The fuel consumption degradation is less than 2% for the considered scenarios. It can be noticed that the first scenario, with a positive offset for the engine torque, shows a more important increase in consumption, whereas the second (negative offset) may lead to a decrease, as it is the case for Artemis urban. This is due to the impact on the stop decision, which may be favored by the latter. Disturbances on SOC have a stronger impact on trajectories where the constraints are active: Artemis urban, $N_\lambda = 10$s and FTP-75, $N_\lambda = 20$s, as it is depicted in Fig. 8. For Artemis urban, the lower constraints are activated during a proportionally longer amount of time than for FTP-75, which explains the difference in the consumption degradation. It can be noticed that SOC limitations are sometimes violated, but this is due to the use of slack variables, as in (15d).

Table 3. Fuel consumption [L/100km] and final SOC[%], different N_λ, T_{ice} offset

Cycle \ Case		Baseline	1	2	3
NEDC	20s	4.87 (70.57%)	4.875 (70.57%)	4.81 (70.57%)	4.86 (70.57%)
	40s	4.76 (70.57%)	4.78 (70.57%)	4.75 (70.57%)	4.77 (70.57%)
A. urban	5s	6.11 (52.58%)	6.115 (52.58%)	6.113 (52.54%)	6.11 (52.68%)
	10s	6.14 (51.15%)	6.15 (51.15%)	6.07 (51.16%)	6.12 (51.16%)
FTP-75	10s	4.82 (57.07%)	4.82 (57.1%)	4.82 (57.1%)	4.82 (57.06%)
	20s	4.82 (55.16%)	4.83 (54.91%)	4.81 (55%)	4.83 (55.04%)
T. jam	10s	6.16 (50.32%)	6.2 (50.33%)	6.17 (50.32%)	6.16 (50.32%)
	20s	6.48 (50.28%)	6.58 (50.29%)	6.5 (50.28%)	6.51 (50.29%)

Table 4. Fuel consumption [L/100km] and final SOC[%], different N_λ, SOC disturbance and combined disturbance (T_{ice} and SOC)

Cycle \ Case		Baseline	4	5
NEDC	20s	4.87 (70.57%)	4.85 (70.33%)	4.85 (70.32%)
	40s	4.76 (70.57%)	4.76 (70.33%)	4.77 (70.32%)
A. urban	5s	6.11 (52.58%)	6.11 (52.26%)	6.11 (52.28%)
	10s	6.14 (51.15%)	6.25 (50.62%)	6.22 (51.04%)
FTP-75	10s	4.82 (57.07%)	4.81 (56.88%)	4.82 (57%)
	20s	4.82 (55.16%)	4.85 (55.9%)	4.83 (55.88%)
T. jam	10s	6.16 (50.32%)	6.2 (50.52%)	6.21 (50.52%)
	20s	6.48 (50.28%)	6.52 (50.53%)	6.54 (50.56%)

6. CONCLUSIONS AND PROSPECTS

In this paper, a two-layer predictive control structure for the energy management of a hybrid electric vehicle was proposed. The MPC low-level controller handles the torque distribution and the engine ON/OFF decision. The latter was introduced without the use of a discrete optimization variable, but as a model-based *a-posteriori* decision. A short-term prediction horizon was used for the MPC problem, which is suitable for real-time implementation and also for reducing the impact of inaccuracies of the linearized prediction model. The MPC cost function translates the trade-off between the engine and the battery use and it was expressed as a weighted sum of the squared consumptions of these two elements. The tuning factor dependence on the drive cycle makes its choice a difficult problem and in this paper, a novel approach was proposed. The tuning is handled at an upper layer, using on a long-term traffic prediction (speed and wheel torque), in an average-based framework, which allows the integration of drive cycle characteristics. The preview horizon should provide a trade-off between transient and average behavior, which is not ensured by an unique value for all types of speed profiles. Here, the wheel power periodogram was introduced in order to define an indicator of the aggressiveness content of the upper layer horizon and thus, providing a tool to determine the horizon value that satisfies the aforementioned requirement.

A sensitivity analysis was also performed, that proved the robustness of the control with respect to SOC and to engine torque estimation. The influence of the driver behavior and of the slope, as well as the introduction of sailing functionality represent topics of a future work.

REFERENCES

Bender, F.A., Uzuner, H., and Sawodny, O. (2014). An adaptive driver model for driving cycle prediction in the intelligent truck. *19th World Congress IFAC*.

Cairano, S.D., Liang, W., Kolmanosky, I., Kuang, M., and Phillips, A. (2011). Engine power smoothing energy management strategy for a series hybrid electric vehicle. *American Control Conf.*

Goerke, D., Bargende, M., Keller, U., Ruzicka, N., and Schmiedler, S. (2015). Optimal control based calibration of rule-based energy management for parallel hybrid electric vehicles. *SAE Tech. Paper*, 2015-01-1220.

Josevski, M. and Abel, D. (2014). Energy management of a parallel hybrid electric vehicles based on stochastic model predictive control. *19th World Congress, IFAC*.

Liu, Z., Ivanco, A., and Filipi, Z. (2015). Quantification of drive cycles rapid speed fluctuations using Fourier analysis. *SAE International*, doi: 10.4271/2015-01-1213.

Lu, Z., Song, J., Yuan, H., and Shen, L. (2013). MPC based torque distribution strategy for energy management of power-split hybrid electric vehicles. *Proc. 32nd Chinese Control Conf.*

Mayr, C.H., Fleck, A., and Jakubek, S. (2011). Hybrid powertrain control using optimization and cycle based predictive control algorithms. *IEEE International Conference on Control and Automation*.

Musardo, C., Rizzoni, G., Guezennec, Y., and Staccia, B. (2005). A-ECMS: an adaptive algorithm for hybrid electric vehicle energy management. *European Journal of Control*.

Ripaccioli, G., Bernardini, D., Cairano, S., Bemporad, A., and Kolmanovsky, I. (2010). A stochastic MPC approach for series hybrid electric vehicle power management. *American Control Conf.*

Sciarretta, A., Guzzella, L., and Back, M. (2004). A real-time optimal control strategy for parallel hybrid vehicles with on-board estimation of the control parameters. *Proc. IFAC Symp. Adv. Automotive Control*.

Stroe, N., Colin, G., Ben-Cherif, K., Olaru, S., and Chamaillard, Y. (2016a). Towards a generic control-oriented model for HEV predictive energy management. *8th IFAC Int. Symp. Advances Automotive Control*.

Stroe, N., Olaru, S., Colin, G., Ben-Cherif, K., and Chamaillard, Y. (2016b). Time-varying MPC-based energy management for hev including engine stop & start. *20th International Conference on System Theory, Control and Computing Joint Conference SINTES 20, SACCS 16, SIMSIS 20*.

Wang, S., Kodagoda, S., and Khushaba, R. (2012). Towards speed-independent road-type classification. *12th International Conference on Control, Automation, Robotics & Vision*.